

### **Accepted manuscript**

As a service to our authors and readers, we are putting peer-reviewed accepted manuscripts (AM) online, in the Ahead of Print section of each journal web page, shortly after acceptance.

### **Disclaimer**

The AM is yet to be copyedited and formatted in journal house style but can still be read and referenced by quoting its unique reference number, the digital object identifier (DOI). Once the AM has been typeset, an ‘uncorrected proof’ PDF will replace the ‘accepted manuscript’ PDF. These formatted articles may still be corrected by the authors. During the Production process, errors may be discovered which could affect the content, and all legal disclaimers that apply to the journal relate to these versions also.

### **Version of record**

The final edited article will be published in PDF and HTML and will contain all author corrections and is considered the version of record. Authors wishing to reference an article published Ahead of Print should quote its DOI. When an issue becomes available, queuing Ahead of Print articles will move to that issue’s Table of Contents. When the article is published in a journal issue, the full reference should be cited in addition to the DOI.

Accepted manuscript  
doi: 10.1680/jemmr.18.00059

---

**Submitted:** 22 June 2018

**Published online in 'accepted manuscript' format:** 14 January 2020

**Manuscript title:** Influence of Glutaraldehyde Cross-linker on Dynamic Properties of Polyvinyl Alcohol Polymer

**Authors:** G. C. Mohan Kumar<sup>1</sup>, P. Jeyaraj<sup>1</sup>, M. Nagamadhu<sup>2</sup>

**Affiliations:** <sup>1</sup>National Institute of Technology Karnataka, Surathkal-575025, India. <sup>2</sup>Acharya Institute of Technology, Bengaluru-560107, India.

**Corresponding author:** G. C. Mohan Kumar, Polymer Composites Laboratory, Mechanical Engineering Department, National Institute of Technology Karnataka, Surathkal-575025, India.

Tel.: +91 824 2473671

**E-mail:** mkumrgc@gmail.com

### **Abstract**

This study investigates the dynamic mechanical properties of Polyvinyl Alcohol (PVA) cross-linked with Glutaraldehyde (GA). The cross-linked polymer is prepared by using a conventional casting technique and then treated with Sulphuric acid for 24 hours. The flexural properties during static and dynamic modes are studied using a three-point bending condition. The static flexural properties improved by adding 30% GA in PVA, with the ductile property. It has observed that dynamic mechanical properties of PVA increase significantly with an increase in cross-linking percentage. The storage and loss modulus increased drastically by adding crosslinker up to 20%, and marginal changes occurred with further addition of crosslinker. The fracture behavior is transformed from ductile to brittle for crosslinker more than 20%. The shifting of rubber region and liquid region with higher temperatures is observed in storage and loss modulus plots. Improvement in adhesion factor, cross-linking density, and effectiveness was observed in GA up to 25%. The test duration is estimated using the Williams-Landel-Ferry model for different temperatures. The major changes are in the modulus in the rubbery plateau region. The cross-linked polymer has a much greater storage and loss modulus indicating the closer network structure and higher stiffness.

**Notation**

$A_f$	Adhesion factor
$C$	Coefficient for effectiveness of crosslinking
DMA	Dynamic Mechanical Analysis
$E'$	Storage Modulus
$E''$	Loss Modulus
$E'_g$	Storage Modulus in glassy region
$E'_r$	Storage Modulus in rubbery region
GA	Glutaraldehyde
$M_c$	Cross-link density
PVA	Polyvinyl Alcohol
$R$	Universal Gas Constant
SEM	Scanning Electron Microscopy
$T$	Test Temperature
$T_g$	Glass Transition Temperature
$T_r$	Room Temperature
TTS	Time-Temperature Superposition
$V_f$	Volume fraction
$Y$	Required years of operation
$\alpha T$	Shift factor
$\Delta E$	Activation energy

## 1. Introduction

Nowadays the world is focussing more on using eco-friendly materials like soy oil-based resin, cellulose fiber, Polylactic Acid (PLA), PVA based fiber and their blended materials in the field of building materials, automobile parts, and civil and construction industries.<sup>1-5</sup> Also, the applications of PVA are having a prominent role in biomedical devices like interference screws, tacks for ligament attachment, meniscal repair, suture anchors, rods, and pins.<sup>6</sup> In this regard, there is a lot of scopes to search for novel bio-materials and is highly pronounced. Thereby the application of bio-materials would help to decrease the global warming effect. Maya and Thomas<sup>7</sup> surveyed in 2008 and reported that bio-materials play a vital role in reducing environmental hazards. Imre et. al.<sup>8</sup> observed that the use of blended biopolymers increased drastically in 2010 onwards, as they have exhibited better performance when compared to base materials. Parinaz et. al.<sup>9</sup> conducted an investigation on Polyvinyl alcohol (PVA) and polyvinyl alcohol/Polyvinyl Pyrrolidone (PVP) bio-medical foams, which are prepared by high-speed mechanical mixing and freeze-drying process. From the study, it is observed that PVA80/20PVP foam had shown better flexibility than pure PVA. It could be due to the uniformly open-pore structure of the prepared materials. Renbo et. al.<sup>10</sup> studied the static and dynamic mechanical properties of PVA fiber reinforced ultra high-strength-strength concrete. From the study, it is revealed that PVA fiber-reinforced concrete showed relatively good ductility, toughness, and deformability when compared to steel-reinforced concrete during static loading conditions. Teresa et al.<sup>11</sup> studied the effect of Cloisite Na<sup>+</sup>, Nanofil (NF) and Cloisite (30B) montmorillonites filler materials for PVA and found that composites with

organically modified montmorillonites exhibited the lowest water absorption as compared to the base materials. Eunsil et al.,<sup>12</sup> worked on lignin/PVA nanocomposites fibers by varying lignin concentrations developed via electro-spinning and concluded that the PVA nanocomposites have advanced functions and they are eco-friendly. Jin and Seungsin<sup>13</sup> demonstrated that polyvinyl alcohol nanofibrous membranes containing Coptidis Rhizoma extracts have considerable potential to ensure the effective antimicrobial wound dressings. Jagadish et al.<sup>14</sup> carried experimentation on proton-conducting solid polymer electrolyte films which are composed of Diazonium Hydrogen Phosphate (DAHP) and PVA. The specimens were prepared by a solution casting method and observed that the addition of nanofillers enhanced the physicochemical properties of DAHP/PVA composites. Shadpour et al.<sup>15</sup> observed that the reinforcement of the Al<sub>2</sub>O<sub>3</sub> nanoparticles with PVA resulted in improvement of thermal properties. In addition, nanoparticle in the polymeric matrix has strong hydrogen bonding between O-H groups of PVA and the O-H groups of the Al<sub>2</sub>O<sub>3</sub> nanoparticles.

Nor et al.<sup>16</sup> studied the mechanical properties of  $\gamma$ -Fe<sub>2</sub>O<sub>3</sub> nanoparticles filled polyvinyl alcohol nanofiber using the electrospinning process. In the study five input variable factors were considered, namely nanoparticles content, voltage, flow rate, spinning distance, and rotating speed to understand the response of Young's Modulus. From the study, it is noticed that about 9% of filler content in PVA had shown the enhanced mechanical properties. Jibril et al.<sup>17</sup> studied the effect of single-walled carbon nanotube nanocomposites and found that incorporation of ozone treatment improved the dispersion of nanoparticle and its interfacial adhesion. Shuai et al.<sup>18</sup> discovered the effect of Calcium Silicate (CaSiO<sub>3</sub>) filler material on the

performance of the PVA materials and found that compressive strength was increased when the filler material is increased by up to 15 weight percent. Elena et al.,<sup>19</sup> worked on Polyvinyl Alcohol/Chitosan (CS)/ montmorillonite (C30B) nanocomposites for food packaging applications and found that mechanical properties improved with 5% weight C30B Nanoclay. Amir et al.<sup>20</sup> examined the influence of PVA content, screw speed, and clay content on the performance of starch/PVA clay nanocomposite films, prepared by twin-screw extruder. From the results, it is observed 5% clay in PVA has exhibited better mechanical properties. Bhasha et. al.<sup>21</sup> observed that 1% Graphene Oxide (GO) content in PVA enhanced the tensile strength and this could be attributed to the existence of hydroxyl and carboxylic groups in PVA and GO nanoparticles, respectively. Yuansen et. al.<sup>22</sup> conducted experiments on leather shaving reinforced PVA composite and found that 5% weight fraction resulted in better tensile strength. Shamima et.al.<sup>23</sup> studied the thermal and mechanical properties of potato starch-filled PVA and PLA composites for biomedical applications. The test results revealed that starch PVA composites have better mechanical properties than pure PVA and starch-filled PLA. Xiaohong et. al.<sup>24</sup> concluded that PVA nanofiber mats cross-linked with glutaraldehyde has exhibited enhanced thermal stability. Subhaakanta et. al.<sup>25</sup> worked on areca fiber reinforced polyvinyl alcohol composite prepared by injection moulding and found that 27% fiber weight fraction exhibited better mechanical property.

From the exhaustive literature review, it is found that biomaterials are the alternatives for environmental hazardous synthetic materials. Moreover, several literatures also focused on enhancing the behavior of PVA by cross-linking with glutaraldehyde and found that, the

cross-linking exhibited a promising enhancement in mechanical and other properties <sup>26, 27</sup>.

However, only limited papers are available on dynamic mechanical properties characterizations of synthetic biodegradable materials. From these published literatures, Polyvinyl Alcohol (PVA) is found to be the most common bio-materials in many applications. This paper focuses on the further characterization of dynamic mechanical properties like adhesion factor, life prediction, cross-linking density, effectiveness, and time-temperature superposition of the biopolymer with cross-linking agent glutaraldehyde.

## 2. Materials and methods

### 2.1 Materials

Polyvinyl Alcohol and Glutaraldehyde are purchased from M/S. Leo Chem India, Bengaluru, India. PVA  $(\text{CH}_2\text{CH}(\text{OH}))_n$  has a molecular weight of 85000 to 124000, with 87 to 89 degrees of hydroxylation <sup>28</sup>. The viscosity of 4% aqueous solution at 20 °C varies from 23 to 38 cps, pH varies from 4.5 to 6.5 and has an ash content maximum of 0.75%. The melting point and boiling points are 200°C and 228°C respectively. The density of PVA is 1.19 g/cm<sup>3</sup>, and Glutaraldehyde  $(\text{OHC}(\text{CH}_2)_3\text{CHO})$  is a 25% aqueous solution having a density of 1.06 g/cm<sup>3</sup>. The GA mixed in PVA for various volume fractions ( $V_f$ ) 5 to 40 to analyze the effect cross-linking on dynamic mechanical properties. The conventional casting technique is used to prepare the biopolymer specimens of 4 mm thickness. The samples prepared are post cured for 24 hours at 60 °C using conventional air oven and then treated with 2 mole of Sulfuric acid ( $\text{H}_2\text{SO}_4$ ) for 24 hours for better cross-linking.



## **2.2 Mechanical properties of PVA-GA**

The bending/flexural strength was evaluated according to ASTM D790 standard. Samples were prepared with a size 12.7 mm width, 127 mm length, and thickness of 4 mm. The experiments were conducted with a crosshead speed of 2 mm/min and a span length of 90 mm. This bending property of PVA and its cross-linked GA polymer were evaluated based on the average value of tests conducted on five identical samples. The dynamic mechanical properties in temperature sweep, of a pure Polyvinyl Alcohol (PVA), and Polyvinyl Alcohol cross-linked with glutaraldehyde (PVA-GA) were measured. Experiments were conducted using a PerkinElmer DMA 8000 model instrument. The experiment uses a three-point bending mode with a Nitrogen flow rate of 20 ml/min. This test is conducted at multi-frequency from 2 Hz to 20 Hz (at intervals of 2 Hz) with temperature scan from 20-180 °C at the heating rate of 2 °C /min and strain rate of 0.050 mm on rectangular samples with a dimension of 50 x 6 x 4 mm. The fracture surfaces of the PVA and its cross-linked samples are analyzed using Scanning Electron Microscopy (SEM) to investigate the fracture morphology and mechanisms.

## **3. Results and discussion**

### *3.1 Mechanical properties*

Initially, the flexural property of the PVA material characterized to understand the effect of the influence of GA on PVA. The percentage of GA is varied from 0% to 40% in steps of 5%, and the corresponding variation in flexural properties is analyzed. The flexural properties were characterized as per the ASTM D790 standard to understand the effect of GA in PVA and

results are shown in Figure 1. As the percentage of GA increases the flexural resistance increases drastically from 10 MPa to 26 MPa, which means relatively inflexible. It clearly shows that there is an improvement of 2.6 times in flexural strength, by adding 30% of GA in PVA. It is due to cross-linking the polymer network, which promotes the breaking and re-forming of bonds can make the polymer stiffer. The flexural strain increases by adding GA up to 15%, further it decreases. It is similar to that of work<sup>21</sup> Graphene Oxide in PVA enhanced the tensile strength, and this could be attributed to the existence of hydroxyl and carboxylic groups in PVA and GO nanoparticles, respectively. The standard deviation (SD) of the flexural strength of each combination shows the level of variation from the average strength reported for five specimens tested. A lower standard deviation indicates that the individual flexural strength of the test specimen tends to closer to the average strength and a higher level of confidence in the average statistical strength reported.

For this statistical report, the maximum variation in the strength is observed at 20%. This clearly shows that 15% GA in the PVA sample allows bending 2.1 times more than the neat PVA. It also may be due to the re-forming of a polymer network and allow deflecting without macro fracture 30. Deflection is more at the bottom surface of the sample compared to the top surface of the sample. The frictional forces generated at the bottom surface are directed toward the mid-span, so as the specimen deflects downward, these frictional forces add to the bending of the specimen. This has a typically a small effect, but can be of concern since there is wear on the test fixture when the specimen slides. This cylinder is placed on the V-groove tightly by springs. The rolling supports eliminate sliding friction and reduce wear. The flexural strength

increases drastically by adding GA in PVA up to 30% and decreases further.

Similarly, good flexural strain behaviour exhibit by adding GA in PVA. It clearly shows that load-carrying capacity increases with the addition of GA and the same composition exhibits favorable bending properties and allows more deformation. This is also noticed in literature that by adding PVA, the flexural fatigue property of composites is improved<sup>31</sup>. It also exhibits good ductility and energy absorption capability. The optimum combinations of GA in PVA were found to be at 30% in flexural mode.

### *3.2 Dynamic mechanical properties*

The storage modulus of the material was measured in the dynamic condition. The energy lost (heat, loss modulus  $E''$ ), the energy recovered (elastic recovery, storage modulus  $E'$ ), and their ratio  $\tan \delta$ . Influence of GA cross-linking on dynamic mechanical properties such as storage modulus, loss modulus, and  $\tan \delta$  is studied. Followed by the extent of GA cross-linking on activation energy, adhesion factor and shift factor is analyzed. Further, the analysis was carried out with a GA cross-linking effect on cross-linking density and cross-linking effectiveness. All these factors will provide a complete characterization of PVA for various proportions of cross-linked with GA.

#### *3.2.1 Storage modulus*

Influence of GA cross-linking and its various volume fraction on storage modulus of PVA is shown in Figure 2. A high storage modulus means that more energy will be recovered. It is clear that the cross-linking enhances the storage modulus of PVA significantly, with an increase

in the volume fraction of GA. It is evident that the enhancement of storage modulus is significant until 20 % GA, and further increase with GA shows a marginal improvement in storage modulus. The variation of storage modulus with respect to temperature can be divided into four different segments for better understanding. The four regions are I. hard plastic region, II leathery region, III. rubber region, and IV. liquid region. In region I, the storage modulus reduces with an increase in temperature, but when compared to other regions, the rate at which the storage modulus decreases with respect to temperature is marginal. This is due to the absence of molecular mobility in the hard plastic state. The storage modulus of this region shows similar behaviour to conventional mechanical properties which is characterized using three-point bending (Section 3.1). The dynamic mechanical properties of PVA cross-linked GA in the hard plastic region shows similar properties during tensile mode also<sup>28</sup>. This is due to the effect of decrease in molecular mobility and increases the degree of cross-linking in the hard plastic region. This may also be due to interlinking by any means (atoms, electrons or ions) between different long backbone chain in a polymer and is called cross-linking. This enhances the binding chain in such a three dimensional way that, the mobility or movement, sliding, breaking of long-chain by the external condition is prevented even at a higher temperature. Cross-linking always enhances the storage modulus by decreasing chain mobility<sup>32, 33</sup>.

Three-point bending is the right technique to identify changes in storage modulus due to changes in cross-linking. The variations of storage modulus with respect to temperature in region II is similar to the region I. However, the rate at which the storage modulus decreases is significant at higher temperature as compared to the region I in general, for all cases. In region

II, it is also observed that the decrease in loss modulus associated with pure PVA is much higher than other GA cross-linked polymer. Similarly, Jibril et al.<sup>17</sup> also reported that the storage modulus of neat PVA decreases drastically at around 80°C. In region II it is also observed that the gap between the storage modulus curve of pure PVA and 5% GA widens with increases in temperature. This clearly indicates that storage modulus increases considerably with increasing in GA in the leathery region. The variation of storage modulus in region III is similar to the variation in the region I and II. But, the rate at which the storage modulus decreases with respect to increase in temperature is less compared to region I. This is due to the mobility of the molecules in the polymer, which creates strain hardening effect with the improvement in the storage modulus<sup>34</sup>. This clearly indicate that cross-linking enhances stiffness (storage modulus) of PVA by cross-linking even at elevated temperature<sup>35</sup>. PVA contains hydroxyl groups (OH)<sup>15,21</sup>, which have the potential to form hydrogen bonds between molecules, resulting in a significant change in surface bond strength between PVA and GA matrix. From region IV, it is observed that an increase in the volume fraction of GA increases storage modulus even at the elevated temperature and this may be due to the reason that, PVA is self-cross-linking due to the high density of hydroxyl groups located on its side chains. It also clears that cross-linking results in bond formation between chains, which decreases chain mobility. The decrease in chain mobility means that chains can't flow past one another upon deformation of the bulk. The chain reaches its mobility limit in smaller deformations, causing the external load to strain the chemical bonds (trying to "bend" them). In case of neat PVA material, the modulus is driven by the difficulty of chains to flow past one another due to

entanglements. Cross-links form a more rigid, non-flowing bulk compared to entanglements. The flexural modulus increases up to 30% even at room temperature testing and further it decreases. A high storage modulus means that more energy will be recovered even at elevated temperature<sup>36</sup>.

By adding 5% of GA, the storage modulus increases by 1.6 times and 12.33 times at 30°C, and 86 °C, respectively. There is a considerable amount of increase in storage modulus at elevated temperature. The same trend of improvement was observed by adding GA in PVA as shown in Figure 2. However, 20% GA addition shows improvement in storage modulus, which increases by 3.29 and 26.17 times at 30°C and 86 °C respectively. Further addition of GA above 20% doesn't show significant improvements in storage modulus for elevated temperatures. The results shows that there is an increase in storage modulus and working temperature by addition of GA. Pure PVA fails at less than 90°C, however, cross-linking with GA elevates it's operating temperature by up to 140°C.

### 3.2.2 Loss modulus

Similar to the storage modulus, loss modulus curves also fall into four different regions. Figure 3 shows that the cross-linking of PVA with GA significantly increases the loss modulus, and it behaves like a storage modulus with temperature. Variations in loss modulus with respect to increasing in temperature at different regions are observed as follows: region I – no significant variations, region II – significant reduction, region III – reduction is not so significant, and region IV – reduction is significant. This clearly shows that by GA cross-linking, energy loss decreases and improves thermal stability even at elevated temperatures. This is due to the

presence of glutaraldehyde as a bifunctional molecule and can react either to other PVA chain yielding a polymer network or to available  $\text{NH}_2$  group from proteins. This GA reaction most probably involves due to the conjugated addition of protein amino groups to ethylene double bonds of  $\alpha$ ,  $\beta$ -unsaturated glutaraldehyde oligomers, since the linkages formed between the protein and glutaraldehyde are irreversible and survive extremes of pH and temperature<sup>37-39</sup>.

As the concentration of cross-linker is increased, there is a movement of the curve towards the lower wavenumber which is observed by Elena et al.<sup>19</sup> using FTIR (Fourier-transform infrared spectroscopy) this identifies the presence of H-bonding. It clears that as the cross-linker reduces the distance between the chains by bridging between them, this bridging leads to lower H-bonding in the material. The presence of two highly reactive alpha protons makes glutaraldehyde more reactive and acidic in nature. The higher reactivity of glutaraldehyde especially at higher dosages leads to a reduction in H-bonding of PVA chains.

Figure 3 shows that adding 5 % GA improves Loss modulus ( $E''$ ) by 2.83 times and 11.28 times at 30 °C and 86 °C respectively. Similarly adding 20% of GA, loss modulus increases by 4.84 times and 24.22 times at 30 °C and 86 °C respectively. This shows that there is an improvement in Modulus by adding GA up to 20% at elevated temperatures. Further variation of  $E''$  value is not so significant with an increase in GA percentage. This improvement in loss modulus may be due to the higher crystallinity content. When PVA is heat-treated, the supplied energy is used to modify the spatial organization of the chains and to establish stronger hydrogen bonding among hydroxyl groups, which leads to a higher crystallinity content. The physical aging of PVA aqueous solutions may cause network formation because of chain

entanglements, especially when the system undergoes heating and post-curing consecutively. On the other hand, the chemically cross-linked polymer was based on the reaction between the cross-linker and the high amount of hydroxyl groups of PVA<sup>15</sup>. Due to this reason the cross-linked polymer exhibit enhances in loss modulus, means energy dissipation or loss is very less. The effect of cross-linking between the hydroxyl groups of PVA and GA is evident that the loss modulus increases shown in Figure 3. The glutaraldehyde has reacted with the hydroxyl groups and thus forming a cross-link.

### 3.2.3 Tan delta

Cross-linker effects on  $T_g$  are difficult to predict, and very different effects were observed. Dynamic mechanical analysis is a sensitive method to determine the  $T_g$ . The incorporation of GA in PVA did not show a distinct effect on  $T_g$ , although a cross-linking of the polymer. The reason is a GA effect, which shifts the  $T_g$  to lower temperatures and acts in opposite direction to the cross-linking effect. Further increase of the GA to 15% or more resulted in a more distinct increase in  $T_g$ . A higher GA loading results in an increase of the cross-linking density of the polymer and to higher  $T_g$  due to decreased chain mobility. The ability of the polymer to dissipate energy decreases as a result of the decreased chain mobility. This is reflected in a decrease of the magnitude of tan delta which is well reproduced in results. Increasing the cross-linking density of the polymer by increasing the GA loading enhances the storage modulus in the rubbery region as can be also seen in Figure 2. The variation of Tan delta with temperature is shown in Figure 4 for various percent of GA on PVA. Tan delta curves are also divided into four regions as discussed in earlier sections.



The peaks of the tan delta are observed in the regions II and III for neat PVA and II, III and IV for cross-linked GA material. These regions quantify the way in which a material absorbs and disperses energy. It is also observed that in the region I material tan delta increases at a faster rate and reaches a maximum peak at the end of the region I. However pure PVA shows maximum peak and it clearly shows maximum material loss factor in pure PVA. The maximum value tan delta corresponding peak temperature shifting to elevated region. This is due to the movements of the PVA chain segments thus became restrained by these cross-linking points of GA, driving the  $T_g$  to higher values<sup>39</sup>. For example, the sample with the highest content of PVA showed the lowest  $T_g$  and was the most flexible. The magnitude of tan delta peak decrease with the association of GA, this may be due to the better cross-linking. In the region II, the variations in tan delta peaks were observed, this may be due to higher viscous up to 10% GA noticed. Further, increase in GA, the glass transition shifting to higher temperature with wider and the slope at which tan delta rise and fall are also wider. This means that the addition of GA in PVA the area under the curve is increasing, which means the material loss factor decreases which are reported in many works of literature<sup>5,28,39</sup>. The area under the curve represents energy required or stored in the material before its failure; this energy is called Modulus of toughness. The second peak is between 119 to 121°C and shows an intimate mix (solubility) between the GA and PVA. From this, it is evident that by adding GA in PVA, the stability will improve even at a higher temperature. In region IV, the material loss factor once again decreases.

The tan delta curve indicates that damping factor can be retained even at elevated

temperature. From the tan delta results, it is evident that two peaks corresponding to two glass transition temperatures are observed due to the presence of GA in PVA, which is also reported in works of literature<sup>39,40</sup>. The cross-link increases the chain length of the PVA and GA, thus the increase in glass transition temperature. This is also evidently observed from the FTIR curves<sup>19</sup>, there is a decrease in H-bonding of the adhesive with a subsequent increase in the amount of cross-linker. A similar trend is observed for  $T_g$ , there is an increase in temperature with increase in the concentration of crosslinker. The crosslinking has been shown by the tan delta curve where there is an evident shift in the peak of the curve towards the higher temperature. This shift in peak is a representation of the transition temperature change which has caused due to the crosslinking of PVA with glutaraldehyde

### 3.2.4 Adhesion factor

Adhesion factor ( $A_f$ ) of a cross-linked polymer refers to the molecular mobility of the polymer matrix. Improved adhesion between constituents of polymer reduces the molecular mobility of the polymer chain. Adhesion factor also used to study the molecular coupling which can occur at the interface and this helps to analyze the way that this coupling can initiate deformation and energy dissipation in the polymer. Adhesion factor can be calculated with the help of dynamic mechanical characterizations of PVA-GA polymer is comparison with pure PVA which is obtained by performing dynamic mechanical analysis of the materials. The expression given by Kubat et al.<sup>41</sup> to calculate the adhesion factor is as follows.

$$\text{Adhesion factor } (A_f) = \left( \frac{1}{1 - V_f} \left( \frac{\tan \delta_c}{\tan \delta_p} \right) \right) - 1 \quad (1)$$

Where,

$V_f$  is volume fraction of GA in PVA.

$\tan \delta_c$  is tan delta value of cross-linking polymer (GA)

$\tan \delta_p$  is tan delta value of polymer (PVA)

The variation of the adhesion factor for various temperatures is shown in Figure 5. From this figure, it is clear that initially the adhesion factor is high and there is a significant variation in adhesion factor up to 35 °C. This can be attributed to the hard-plastic region and the absence of molecular mobility and hence adhesion factor is high. But the magnitude of adhesion factor increases with respect to the cross-linking percentage for GA more than 25%. As the temperature increases, the adhesion factor decreases drastically at around 40 °C and reaches a negative value at around 45°C. This is due to the temperature and frequency is sententious increases up to a certain point say 40 °C the bonding between the PVA and GA are weaker due to the viscoelastic behaviour 42. This is maybe due to the molecular stick-slip phenomena between PVA and GA. At 50°C it reaches the lowest value, which shows weaker adhesion between GA to PVA. However, the variation of the adhesion factor is marginal from 50°C to 80°C and magnitude of adhesion factor increases with an increase in GA cross-linking percentage. The variation of adhesion factor of 40% GA in PVA polymer is much significant and it shows only positive value.

This indicates by adding GA, stiffness of the polymer increases and adhesion between two polymers is also improves <sup>34</sup>. This, in turn, maintains constant bonding factor which can also be seen in Figures 2 & 3 in the region - I. Hence, there is a strong adhesion between GA

and PVA polymers at ambient temperature.

### 3.2.5 Activation energy

Activation energy is the minimum energy that is required to initiate a chemical reaction.

Activation energy analysis was carried out to further understand the thermo-mechanical response of pure PVA and PVA-GA composites.<sup>43,44</sup>

$$\text{Activation Energy} = \Delta E = 2.305 \times R \times \frac{d(\log f)}{d\left(\frac{1}{T}\right)} \quad (2)$$

Where,

R is Universal gas constant 8.134 J/mol-K.

$d(\log f)$  and  $d(1/T)$  is the slopes from the activation energy plot.

By substituting slope data from Table 1 (from Figure 6) in equation 2, the activation energy was computed and noted in Table 1. The pure PVA shows 63.14 kJ/mol<sup>45,46</sup> by cross-linking the significant improvement due to the addition of GA in PVA and maximum activation energy shows at 20%.

### 3.2.6 Estimation of the operating life of PVA-GA polymer

The linear relation between  $\log f$  versus  $1/T$ , observed during the activation energy analysis for pure PVA and PVA-GA polymer suggested that these material exhibit Arrhenius relationship and that the Williams-Landel-Ferry model<sup>47,48</sup> given below, which can be applied to determine the shift factor.

$$\text{Shift factor for temperature} < T_g = aT = \exp \frac{\Delta E}{R} \left[ \frac{1}{T} - \frac{1}{T_r} \right] \quad (3)$$

Where,

T is Test Temperature in K

R is Universal Gas Constant in KJ/mol K

T<sub>r</sub> is Room Temperature in K

ΔE is Activation energy in kJ/mol

The Time-Temperature Superposition (TTS) is used to determine the accelerated test conditions to estimate the operational life of polymer and its composites since these materials undergo time-dependent decay in properties. For example, if the properties of 20% PVA-GA part after 10 years of operation under ambient conditions are required, then accelerated tests can be conducted at 70 °C and 100 °C. The test duration can be computed using Equation 3 and the shift factor is taken from Figure 7 corresponding to pure PVA and PVA-GA polymer. The computed estimated test duration is 35 days at 70 °C and 2 days at 100 °C respectively. Similarly, the calculation was performed for different GA percentages and results are shown in Figure 8. From the figure, it is evident that cross-linked PVA with GA has a higher operational life than pure PVA. As the operating temperature is higher the test duration decreases to predict the life of the material. Figure 8 shows a testing duration concerning temperature and GA cross-linking.

$$\text{Test Duration} = 365 \alpha T Y \quad (4)$$

Where,

Test duration in days

αT is shift factor

Y is required years of operation of the polymer at ambient temperature.

### 3.2.7 Crosslinking density ( $M_c$ )

The cross-linking density is determined using dynamic mechanical analysis <sup>49,50</sup>. In this case, evaluations are performed under low deformations (<100 %) and  $M_c$  is calculated from experimental results. The  $M_c$  is cross-link density as the inverse of the molecular volume between cross-links for chemically cross-linked polymers is given by

$$\frac{M_c}{\rho} = \frac{3RT}{E'} \quad (5)$$

Where

$E'$  is Storage Modulus in GPa.

$R$  is universal gas constant.

$T$  is the temperature in K near  $T_g$ .

Figure 9 shows the cross-linking density of PVA-GA polymer, by adding Glutaraldehyde the cross-linking density increases up to 25%, further it decreases and maintains stagnant behavior up to 40%. This is also evident in storage modulus, loss modulus, adhesion factor, and shift factor. From this, it is clear that 20 to 25% GA cross-linked polymer is stiffer than other compositions even at elevated temperature<sup>34</sup>. This is directly related to the extent of cross-linking, the higher the degree of cross-linking the greater the storage modulus.

### 3.2.8 Effectiveness

The effectiveness of cross-linking on the modulus of the polymer can be represented by a coefficient  $C$  such as <sup>51,52</sup>.

$$C = \frac{\frac{E'_g}{E'_r} PVA - GA}{\frac{E'_g}{E'_r} PVA} \quad (6)$$

Where

$E'_g$  and  $E'_r$  are the storage modulus values in the glassy and rubbery region respectively.

Higher the value of constant  $C$ , lower the effectiveness of the glutaraldehyde cross-linking. The value of  $E'_g$  and  $E'_r$  is used at 30°C and 80°C in case of pure PVA, similarly the value  $E'_g$  is used at 30 °C and  $E'_r$  is used at 70, 80 and 90°C of PVA-GA for better understanding of effectiveness. The values obtained for the different cases at frequency 10 Hz are given in Table 2. In this case, the lowest value is obtained at 15% of GA at 70°C, less than 20% GA at 80 °C. It is important to note that the modulus in the glassy state is determined primarily by the strength of the intermolecular forces and the way the polymer chain is packed.

### 3.2.9 Deflection

To understand how PVA cross-linked polymer respond to bending force, the bending strain is applied at the middle of the span length and noted the deflection over a range of temperature. Similarly like earlier sections the deflection - temperature responses curve divided into four regions to facilitate the analysis of the mechanical response of the cross-linked polymer. The effect of deflection (microns) with temperature for GA cross-linking is shown in Figure 10. Region I: negligible change in deflection, this is due to hard plastic state at a lower temperature. So very difficult to identify the influence of GA in PVA. In region II, as the temperature increases the energy lost from the sample, and leads to losses of its stiffness. This behavior also

observed in storage and loss modulus plots refers to significant change. Whereas in pure PVA, the material becomes soft at higher temperatures and further material may not sustain any load. The softening is also observed in storage modulus and loss modulus curves in earlier sections. It is also observed that the increase in deflection associated with pure PVA is much higher than other GA cross-linked polymer. By adding 5% of GA the value of deflection decreases drastically and reaches stagnant level at the end of this region. In region III, no such change in deflection is observed it is almost constant in nature for both pure PVA and cross-linked polymers. In region IV, the pure don't withstand any further stain and fails to work under dynamic conditions. By adding GA the thermal stability of PVA improved to a greater extent and dynamic operating temperature is also enhanced. It is also observed that small variations in the deflection curve at a higher temperature. This clearly indicates that cross-linking enhances stiffness 34 of PVA even at elevated temperatures.

### *3.3 Microstructure of fractured surface*

The fracture morphology of PVA/PVA-GA samples are analysed for both static flexural test (three-point bending) and thermo-mechanical (dynamic mechanical analysis) cases.

In flexural mode, the point load is applied at the mid of the sample, and the top surface is subjected to compression and the bottom surface is subjected to tension. So fractured images are analyzed at the bottom surface to understand the behaviour. Figure 11 shows the fractured images of static flexural testing. Ductile failure is observed in both 15% and 20% GA in PVA polymers, and their fracture morphology is shown in Figure 11a) and b). This is evident in the flexural stress-strain graph discussed in section 3.1. As the percentage of GA increases more



than 20% the ductile fracture is converted to brittle fracture as shown in Figure 11c) and d).

Figure 12 shows the SEM images of dynamic mechanical analyses samples. In dynamic working condition, the samples are exposed in a loading frequency (1 to 20Hz) and temperature (30-180°C). It is necessary to understand the morphology after the test. Figure 12 a) shows the morphology of PVA samples, small crack is observed and failure occurs within 90°C. Figure 12 b) shows the morphology of 20% GA in PVA sample and it is observed that samples sustain the load in elevated temperature. Figure 12 c) shows the fractured surface of 30% GA in PVA samples, and a brittle crack was found after exposure to 180°C of working condition. Figure 12 d) shows fracture images of 40% GA in PVA sample and brittle nature of the failure. From these morphology studies, it is concluded that between 15 to 25% GA in PVA exhibit ductile fracture. If GA increases to more than 25%, the ductile fracture is converted into a brittle fracture.

#### **4. Conclusion**

The Polyvinyl Alcohol behaviour in Dynamic Mechanical Analysis with respect to temperature, frequency and cross-linking effect of glutaraldehyde are studied and concluded that,

1. Mechanical properties studied in flexural mode exhibit better-bending properties with excellent ductile and energy absorption behaviour at up to 30% GA.
2. Storage modulus increases with an increase in the percentage of Glutaraldehyde up to 20% at room temperature and at also elevated temperature. The Loss modulus also improved by adding glutaraldehyde even at elevated temperature.
3. Shift factor and Activation Energy are determined to estimate the life cycle of PVA.

The cross-linked polymer of all the GA cases shows enhanced behaviour and hence the strength is found to be dependent on the composition of the cross-linking. Equations are proposed on the Williams-Landel-ferry model, is used to predict the testing duration for different cross-linked polymers at different working temperature.

4. Adhesion factor, effectiveness index, and cross-linking density are improved favorably by GA addition.
5. Cross-linked polymers are important because they are mechanically strong and resistant to heat.

From these results, it is concluded that PVA cross-linked with GA up to 20% considerably enhances the Storage and Loss modulus, also the other properties considerably even at elevated temperatures.

## References

1. T. Gurunathan, S. Mohanty, and S. K. Nayak (2015) A review of the recent developments in biocomposites based on natural fibres and their application perspectives. *Composites: Part A Applied Science and Manufacturing* **77**: 1–25.
2. M. A. Dweib, B. Hu, H. W. Shenton, and R. P. Wool (2006) Bio-based composite roof structure: Manufacturing and processing issues. *Composite Structures* **74**: 379-388.
3. G. Koronis, A. Silva, and M. Fontul (2013) Green composites: A review of adequate materials for automotive applications. *Composite Part B: Engineering* **44 (1)**: 120-127.
4. J. Qiu, X. Lim, and E. Yang (2016) Cement and Concrete Research Fatigue-induced deterioration of the interface between micro-polyvinyl alcohol (PVA) fiber and cement matrix. *Cement and Concrete Research* **90**: 127–136.
5. Amaresh Gunge, Praveennath G. Koppad, M. Nagamadhu, S. B. Kivade, and K.V. Shivananda Murthy (2019) Study on mechanical properties of alkali treated plain woven banana fabric reinforced biodegradable composites. *Composite Communication* **13**: 47-51.
6. J. C. Middleton and A. J. Tipton (2000) Synthetic biodegradable polymers as orthopedic devices. *Biomaterials* **21**: 2335-2346.
7. M. J. John and S. Thomas (2008) Biofibres and biocomposites. *Carbohydrate Polymers* **71**: 343-364.
8. B. Imre and B. Pukánszky (2013) Compatibilization in bio-based and biodegradable polymer blends. *European Polymer Journal* **49**: 1215-1233.
9. Parinaz Sabourian, Masoud Frounchi and Susan Dadbin (2017) Polyvinyl alcohol and

- polyvinyl alcohol/polyvinyl pyrrolidone biomedical foams crosslinked by gamma irradiation. *Journal of Cellular Plastics* **53(4)**: 359–372.
10. Renbo Zhang, Liu Jin, Yudong Tian, Guoqin Dou, Xiuli Du (2019) Static and dynamic mechanical properties of eco-friendly polyvinyl alcohol fiber-reinforced ultra-high-strength concrete. *Structural Concrete* **1–13**. DOI: 10.1002/suco.201800247
11. Teresa M Pique, Claudio J Pe´rez, Vera A Alvarez and Analı´a Va´zquez (2014) Water soluble nanocomposite films based on poly(vinyl alcohol) and chemically modified montmorillonites. *Journal of Composite Materials* **48(5)**: 545–553.
12. Eunsil Lee, Youjung Song and Seungsin Lee (2019) Crosslinking of lignin/poly(vinyl alcohol) nanocomposite fiber webs and their antimicrobial and ultraviolet-protective properties. *Textile Research Journal* **89(1)**: 3–12.
13. Jin Jeong and Seungsin Lee (2018) Electrospun poly(vinyl alcohol) nanofibrous membranes containing Coptidis Rhizoma extracts for potential biomedical applications, *Textile Research Journal* **1-13**. <https://doi.org/10.1177/0040517518813679>.
14. Jagadish Naik, RF Bhajantri, Sunil G Rathod and Ishwar Naik (2019) Proton conducting diazonium hydrogen phosphate/poly(vinyl alcohol) electrolytes: Transport, electrical, thermal, structural, and optical properties. *Journal of Elastomers & Plastics* **51(5)**: 390–405.
15. Shadpour Mallakpour and Mohammad Dinari (2013) Enhancement in thermal properties of poly(vinyl alcohol) nanocomposites reinforced with Al<sub>2</sub>O<sub>3</sub> nanoparticles. *Journal of Reinforced Plastics and Composites* **32(4)**: 217–224

16. Nor Hasrul Akhmal Ngadima, Noordin Mohd Yusof, Ani Idris, Denni Kurniawan and Ehsan Fallahiarezoudar (2017) Fabricating high mechanical strength  $\gamma$ -Fe<sub>2</sub>O<sub>3</sub> nanoparticles filled poly(vinyl alcohol) nanofiber using electrospinning process potentially for tissue engineering scaffold. *Journal of Bioactive and Compatible Polymers* **32(4)**: 411–428.
17. Jibril Al-Hawarin, Ayman S Ayesh and Essam Yasin (2013) Enhanced physical properties of poly(vinyl alcohol)-based single-walled carbon nanotube nanocomposites through ozone treatment of single-walled carbon nanotubes. *Journal of Reinforced Plastics and Composites* **32(17)**: 1295–1301.
18. Ci-jun Shuai, Zhong-zheng Mao, Zi-kai Han and Shu-ping Peng (2014) Preparation of complex porous scaffolds via selective laser sintering of poly(vinyl alcohol)/calcium silicate. *Journal of Bioactive and Compatible Polymers* **29(2)**: 110–120.
19. Elena Butnaru, Catalina Natalia Cheaburu, Onur Yilmaz, Gina Mihaela Pricope and Cornelia Vasile (2016) Poly(vinyl alcohol)/chitosan/ montmorillonite nanocomposites for food packaging applications: Influence of montmorillonite content. *High Performance Polymers* **28(10)**: 1124–1138.
20. Amir H Navarchian, Mehdi Jalalian and Majid Pirooz (2015) Characterization of starch/poly(vinyl alcohol)/clay nanocomposite films prepared in twin-screw extruder for food packaging application. *Journal of Plastic Film & Sheeting* **31(3)**: 309–336.
21. Bhasha Sharma, Parul Malik, Purnima Jain (2019) To study the effect of processing conditions on structural and mechanical characterization of graphite and graphene

- Oxide-reinforced PVA nanocomposite. *Polymer Bulletin* **76**: 3841–3855.
22. Yuansen Liu, Qi Wang and Li Li, (2016) Reuse of leather shavings as a reinforcing filler for poly (vinyl alcohol). *Journal of Thermoplastic Composite Materials* **29(3)**: 327–343.
23. Shamima Eaysmine, Papia Haque, Taslima Ferdous, Md Abdul Gafur and Mohammed M Rahman (2016) Potato starch-reinforced poly(vinyl alcohol) and poly(lactic acid) composites for biomedical applications. *Journal of Thermoplastic Composite Materials* **29(11)**: 1536–1553.
24. Xiaohong Qin, Guanxian Dou, Guojun Jiang and Sai Zhang (2013) Characterization of poly (vinyl alcohol) nanofiber mats cross-linked with Glutaraldehyde. *Journal of Industrial Textiles* **43(1)**: 34-44.
25. Subhakanta Nayak and Jyoti Ranjan Mohanty (2019) Study of Mechanical, Thermal, and Rheological Properties of Areca Fiber-Reinforced Polyvinyl Alcohol Composite. *Journal of Natural Fibers* **16(5)**: 688–701.
26. Y. Wang and Y. Lo Hsieh (2010) Crosslinking of polyvinyl alcohol (PVA) fibrous membranes with glutaraldehyde and peg diacylchloride. *Journal of Applied Polymer Science* **116**: 3249-3255.
27. R. Rudra, V. Kumar, and P. P. Kundu (2015) Acid catalysed cross-linking of polyvinyl alcohol (PVA) by glutaraldehyde: effect of crosslink density on the characteristics of PVA membranes used in single chambered microbial fuel cells. *RSC Advances* **5(101)**: 83436–83447. doi:10.1039/c5ra16068e.
28. G.C. Mohan Kumar, P. Jeyaraj, M. Nagamadhu (2019) Dynamic mechanical analysis of

- glutaraldehyde cross-linked polyvinyl alcohol under tensile mode. *AIP Conference Proceedings* 020017, 2057 (1).
29. Amaresh Gunge, Sangshetty Bheemanna Kivade, Mahadevappa Nagamadhu, Sangamesh Rajole (2019) Mechanical properties of chemically treated woven banana/polyvinyl alcohol composites. *Emerging Materials Research* **8(4)**: 1-6.
30. Saori Sasaki and Atsushi Suzuki (2014) Change in molecular weight distribution by elution of polymers from PVA cast gel. *Polymer Bulletin* **71(9)**: 2383–2394.
31. Meng D, Lee CK, Zhang Y (2019) Flexural fatigue properties of a polyvinyl alcohol-engineered cementitious composite. *Magazine of Concrete Research* **71(21)**: 1130-1141. <https://doi.org/10.1680/jmacr.18.00197>
32. J. V Cauich-Rodriguez, S. Deb, R. Smith (1996) Effect of cross-linking agents on the dynamic mechanical properties of hydrogel blends of poly(acrylic acid)- poly(vinyl alcohol-vinyl acetate). *Biomaterials* **17 (23)**: 2259-2264.
33. A. K. Sonker, H. D. Wagner, R. Bajpai, R. Tenne, and X. M. Sui (2016) Effects of tungsten disulphide nanotubes and glutaric acid on the thermal and mechanical properties of polyvinyl alcohol. *Composite Science of Technology* **127**: 47–53.
34. J. Richeton, G. Schlatter, K. S. Vecchio, Y. Rémond, and S. Ahzi (2005) A unified model for stiffness modulus of amorphous polymers across transition temperatures and strain rates. *Polymer (Guildf)* **46**: 8194-8201.
35. A. Romo-Uribe, JA Arcos-Casarrubias, A Reyes-Mayer, and R Guardian-Tapia (2017) PDMS anodomains in DGEBA epoxy resin induce high flexibility and toughness.

*Polymer Plastics Technology Engineering* **56**: 96-107.

36. Shin J, Nouranian S, Ureña-Benavides EE and Smith AE (2017) Dynamic mechanical and thermal properties of cellulose nanocrystal/epoxy nanocomposites. *Green Materials* **5(3)**: 123–134. <http://dx.doi.org/10.1680/jgrma.17.00005>
37. A.M. Araujo, M.T. Neves Jr., W.M. Azevedo, G.G. Oliveira, D.L. Ferreira Jr., R.A.L. Coelho, E.A.P. Figueiredo and L.B. Carvalho Jr. (1997) Polyvinyl alcohol-glutaraldehyde network as a support for protein immobilization. *Biotechnology Techniques* **11(2)**: 67–70.
38. Katia C. S. Figueiredo, Tito L. M. Alves, Cristiano P. Borges (2009) Poly(vinyl alcohol) Films Crosslinked by Glutaraldehyde Under Mild Conditions. *Journal of Applied Polymer Science* **111**: 3074–3080.
39. Uma Thanganathan, Masayuki Nogami (2014) Influence of glutaraldehyde cross-linking with polymer/heteropolyacid membranes. *Emerging Materials Research* **3(2)**: 85-90.
40. A. Romo-Uribe, K Santiago-Santiago, A Reyes-Mayer, and M Aguilar-Franco (2017) Functional PDMS enhanced strain at fracture and toughness of DGEBA epoxy resin. *European Polymer Journal* **89**: 101-118.
41. J. Kubt, M. Rigdahl, and M. Welander (1990) Characterization of interfacial interactions in high density polyethylene filled with glass spheres using dynamic mechanical analysis. *Journal Applied Polymer Science* **39 (7)**: 1527-1539.
42. Xiaohui Zhang, Haifang Liu, Jinmin Qin, Xueqiong Yin, Ju Lv, Li Zhu (2017) Preparation and platelet adhesion of chitosan/PVA nanofibrous membrane. *Bioinspired, Biomimetic and Nanobiomaterials* **6(4)**: 199-207.



43. N. A. Fauziyah, T. A. Fadly, A. Rosyidi, Mashuri, and S. Pratapa (2017) Activation energy determination in multi-frequency dynamic molecular interaction analysis of PEG 4000-Cristobalite composites using DMA. *Journal of Physics: Conference Series* **817**: 012020.
44. A. Rudin and P. Choi (2013) *The Elements of Polymer Science and Engineering*. 3rd edition, *Academic Press*, **1- 584**.
45. N. Khalifa, H. Kaouach, W. Zaghdoudi, M. Daoudi, and R. Chtourou (2015) Photoluminescence investigations and thermal activation energy evaluation of Fe<sup>3+</sup> -doped PVA films. *Applied Physics A: Materials Science & Processing* **120**: 1469-1474.
46. D. zhan Ye, X. Zhang, S. Gu, Y. Zhou, and W. Xu (2017) Non-isothermal crystallization kinetics of eucalyptus lignosulfonate/polyvinyl alcohol composite. *International Journal of Biological Macromolecules* **97**: 249-257.
47. Liu, C., Lu, H., Li, G., Hui, D., and Fu, Y. Q. Richard (2019) A cross-relaxation effects model for dynamic exchange of water in amorphous polymer with thermochemical shape memory effect. *Journal of Physics D: Applied Physics* **52**: 345305. doi:10.1088/1361-6463/ab2860.
48. Williams M L, Landel R F and Ferry J D (1955) The Temperature Dependence of Relaxation Mechanisms in Amorphous Polymers and Other Glass-forming Liquids. *Journal of the American Chemical Society* **77(14)**: 3701-3707.
49. Z. Xia, M. Patchan, J. Maranchi, J. Elisseeff, and M. Trexler (2013) Determination of crosslinking density of hydrogels prepared from microcrystalline cellulose. *Journal of*

*Applied Polymer Science* **127** (6): 4537-4541.

50. K. Berean, Jian Zhen Ou, Majid Nour, Kay Latham, Chris McSweeney, David Paull, Andri Halim, Sandra Kentish, Cara M. Doherty, Anita J.Hill, and Kourosch Kalantar-zadeh (2014) The effect of crosslinking temperature on the permeability of PDMS membranes: Evidence of extraordinary CO<sub>2</sub> and CH<sub>4</sub> gas permeation. *Separation and Purification Technology* **122**: 96-104.
51. L. A. Pothan and S. Thomas (2003) Polarity parameters and dynamic mechanical behaviour of chemically modified banana fiber reinforced polyester composites. *Composite Science Technology* **63**: 1231-1240.
52. L. Pothan, Z. Oommen, and S. Thomas (2003) Dynamic mechanical analysis of banana fiber reinforced polyester composites. *Composite Science Technology* **63**: 283-293.

**Table 1.** Slope data from Figure 6

Samples	1 <sup>st</sup> Slope d(log f)/d(1/T)	R <sup>2</sup>	$\Delta E$ in KJ/mol 1 <sup>st</sup> slop
Pure PVA	3297.8	0.9096	63.143
5%	3425	0.9944	65.579
10%	3827.6	0.9666	73.288
15%	4002	0.9535	76.626
20 %	5262.3	0.9891	100.76
25 %	4359.5	0.9875	83.472

**Table 2.** Effectiveness of crosslinking agent

% GA	C at 70 °C	C at 80 °C	C at 90 °C
5 %	0.332	0.176	0.081
10 %	0.339	0.177	0.079
15 %	0.296	0.178	0.089
20 %	0.316	0.178	0.081
25 %	0.346	0.200	0.086
30 %	0.331	0.183	0.077
35 %	0.326	0.192	0.088
40 %	0.428	0.256	0.121

**Figure 1.** Flexural strength and strain for various percentage of GA in PVA

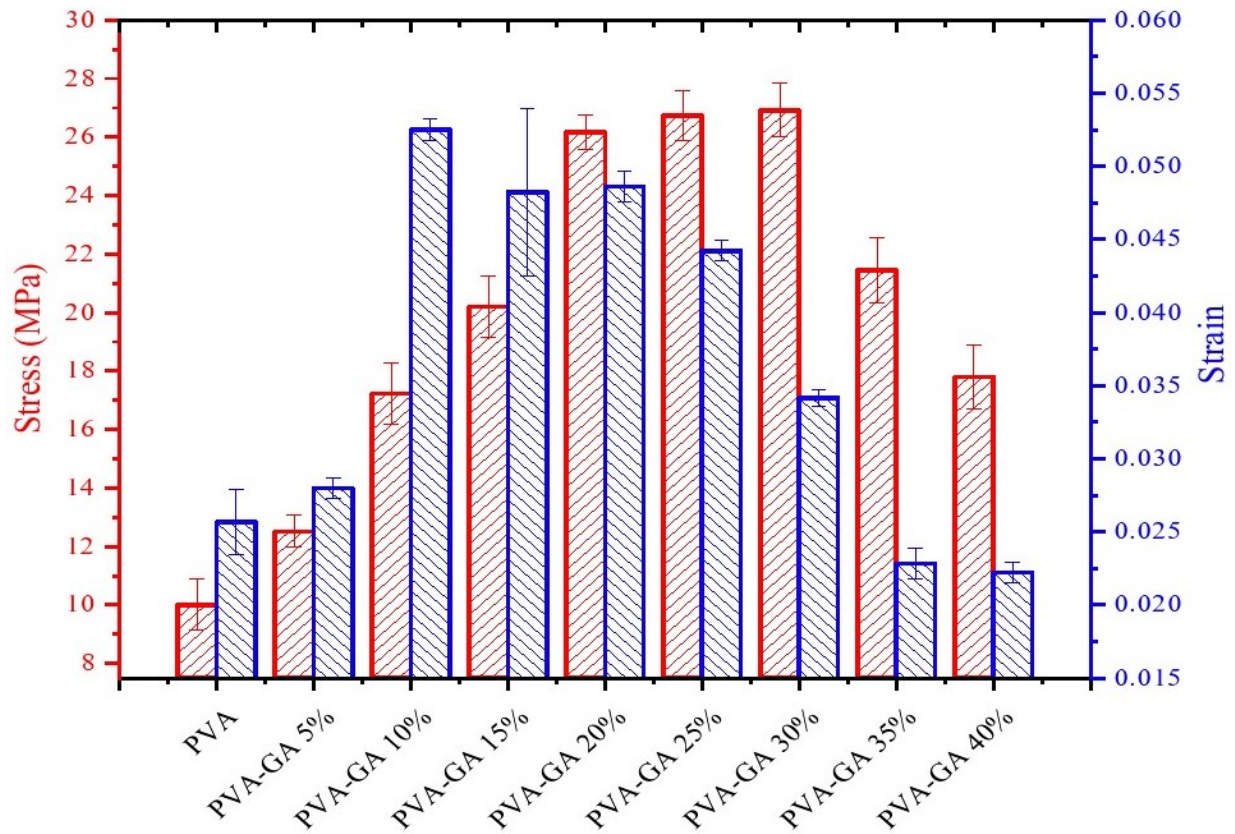


Figure 2. Variation of storage modulus for various percentage of GA in PVA

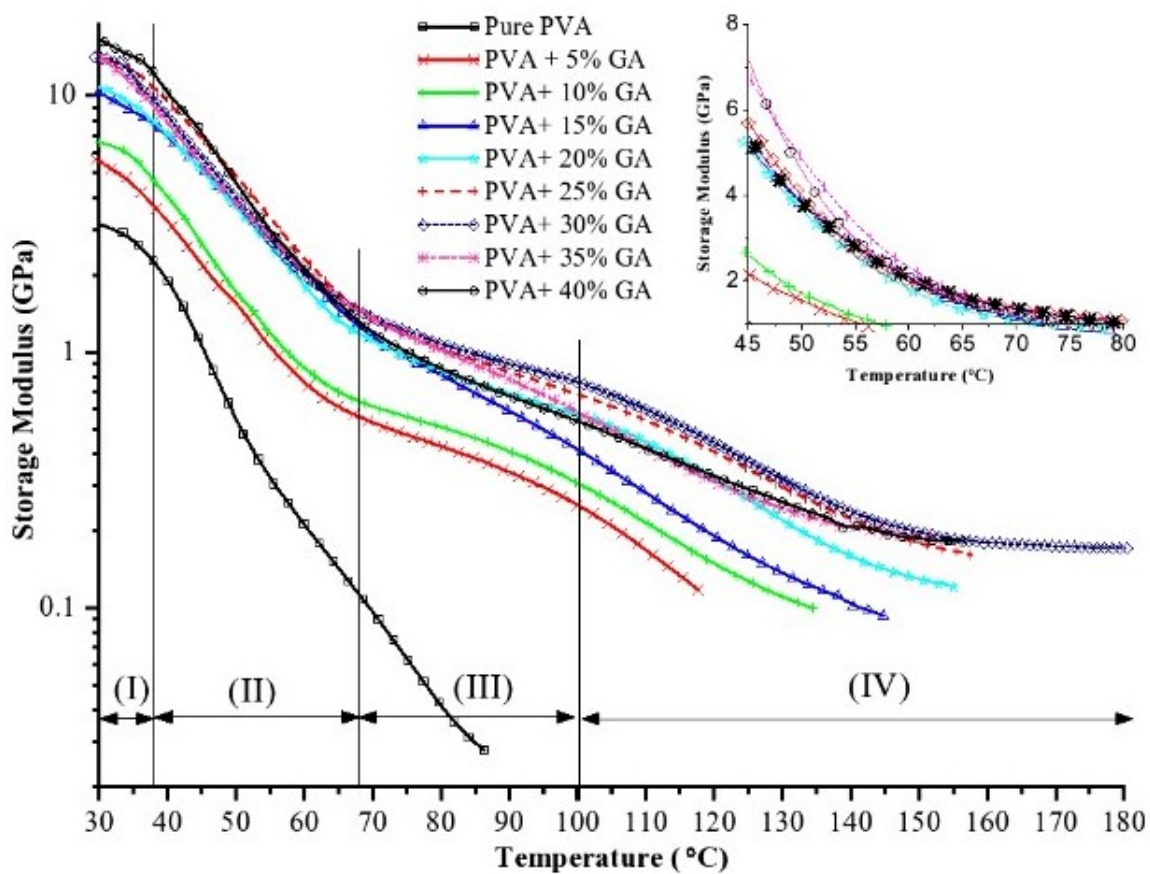
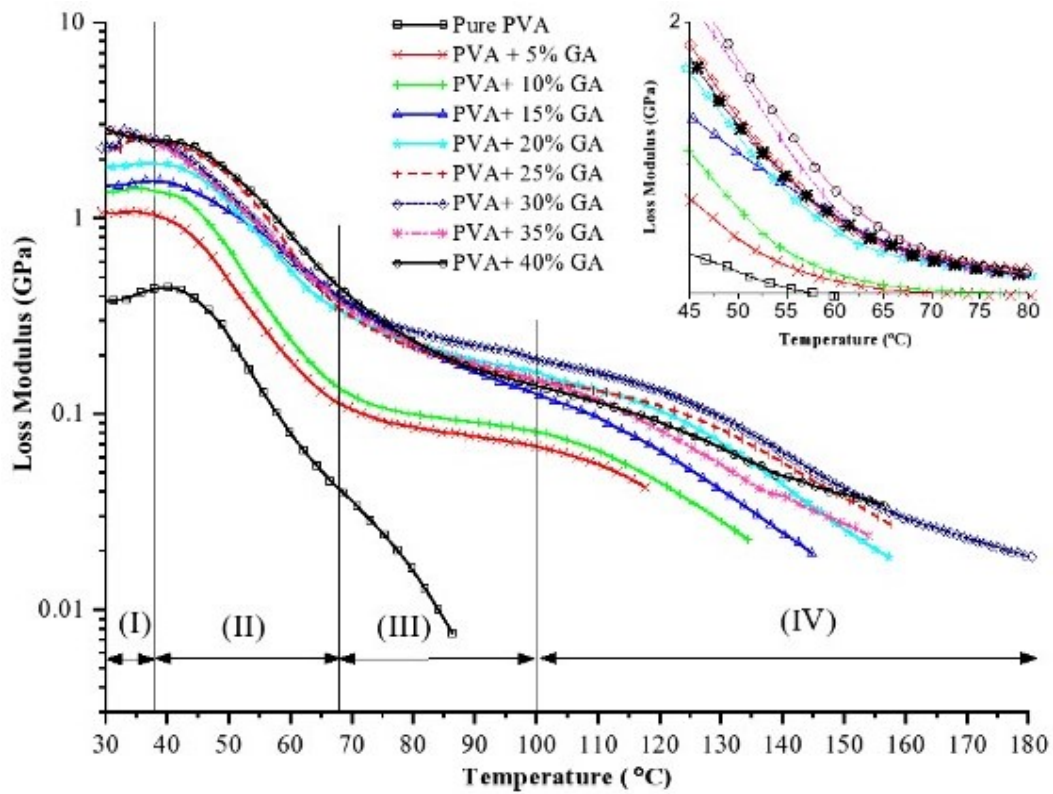


Figure 3. Influence of GA crosslinking on loss modulus



**Figure 4.** Influence of GA crosslinking on Tan delta

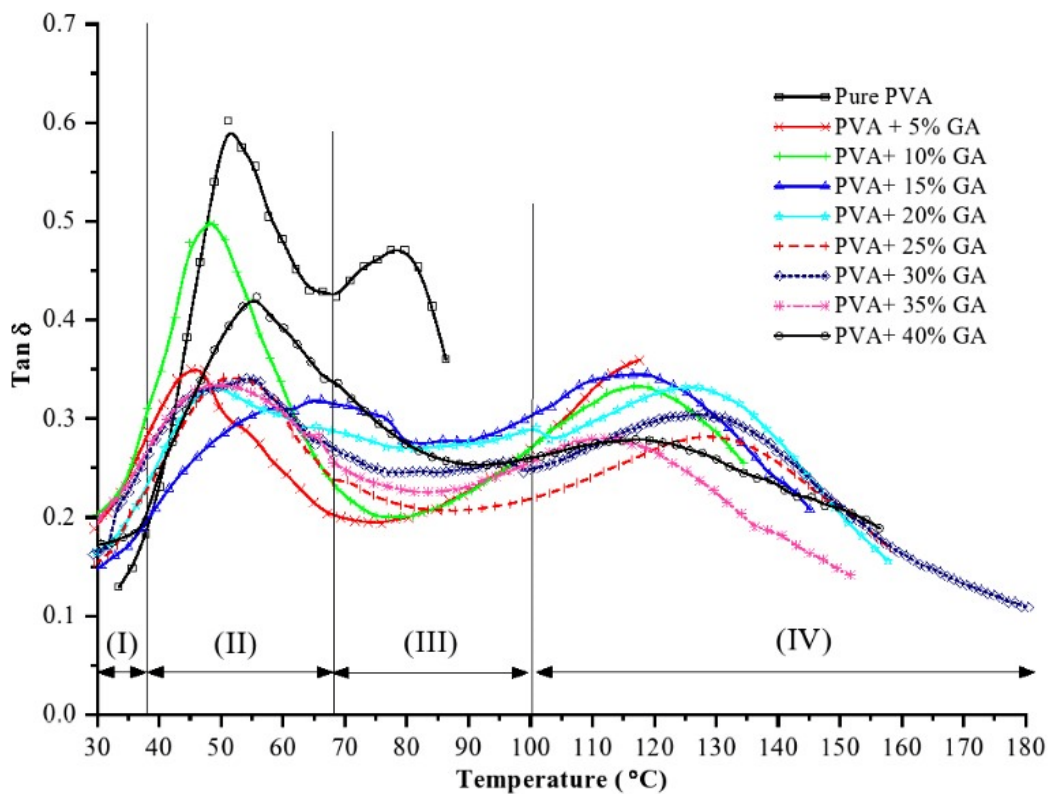




Figure 5. Influence of crosslinking percentage of GA on adhesion factor

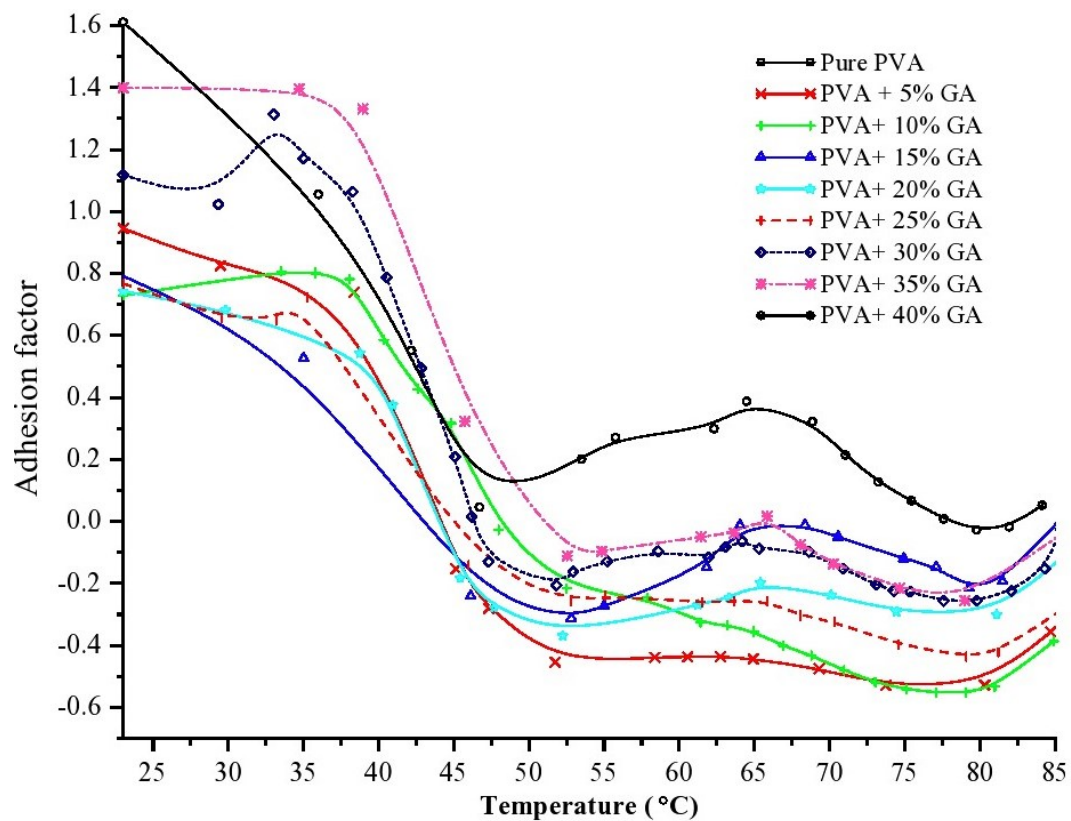


Figure 6. Log frequency plot for pure PVA and various percentage of GA

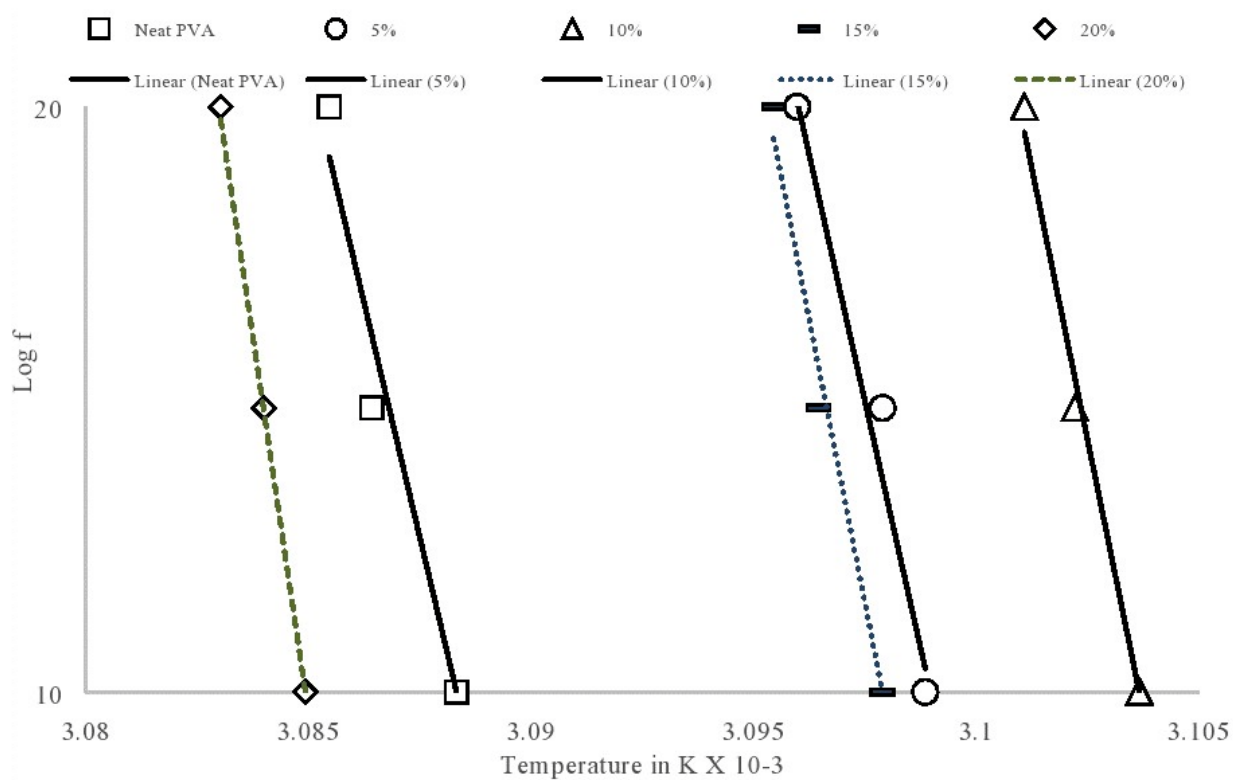
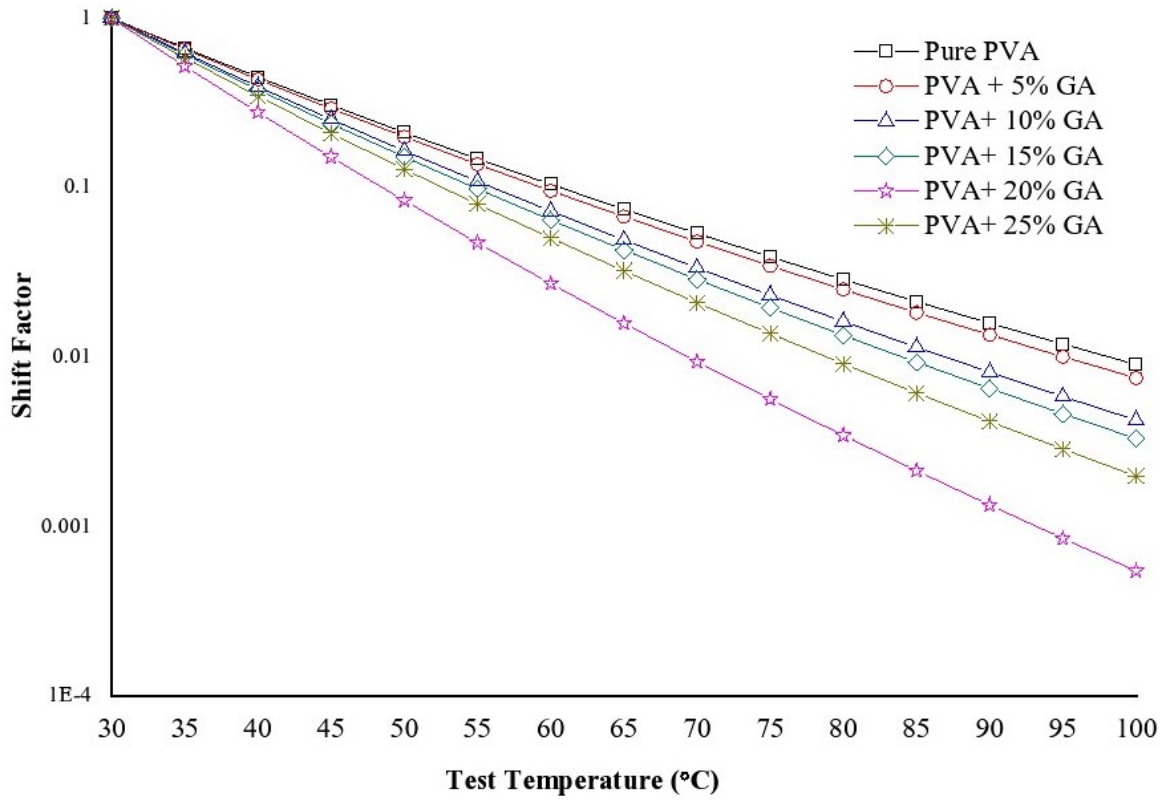
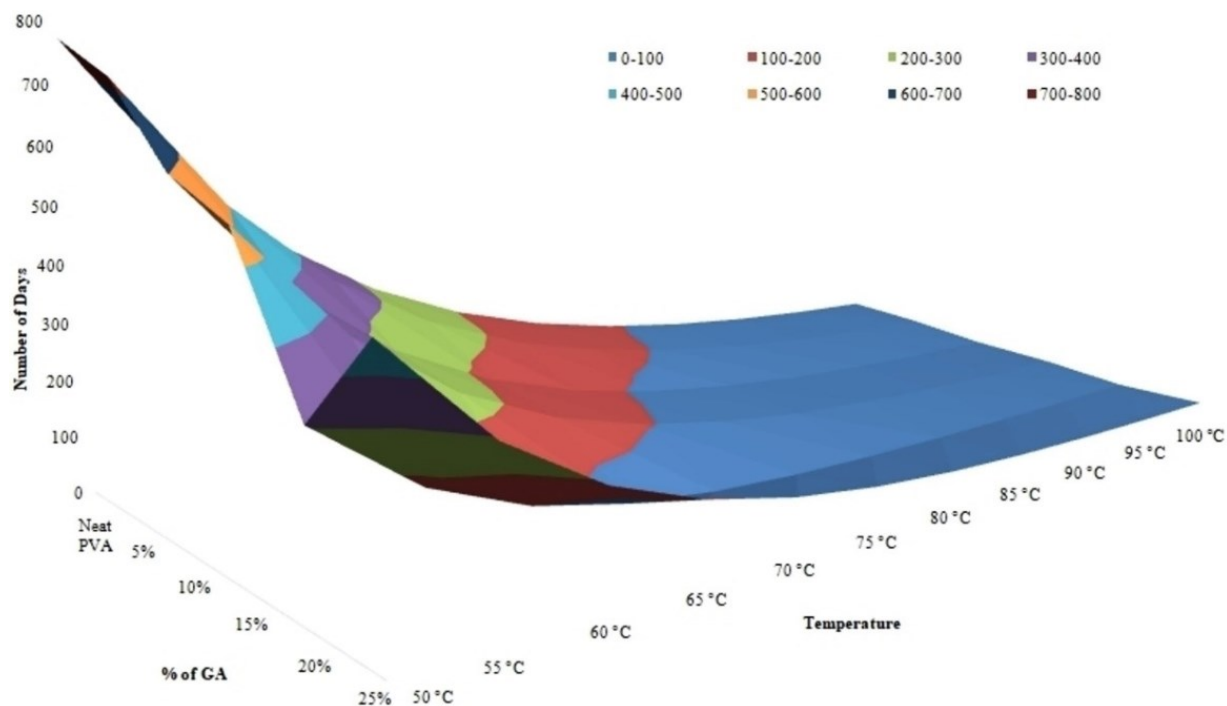


Figure 7. Shift factor for time-temperature superposition (TTS) analysis



**Figure 8.** Test duration in days for pure PVA and PVA-GA at different temperatures



**Figure 9.** Crosslinking density of PVA-GA

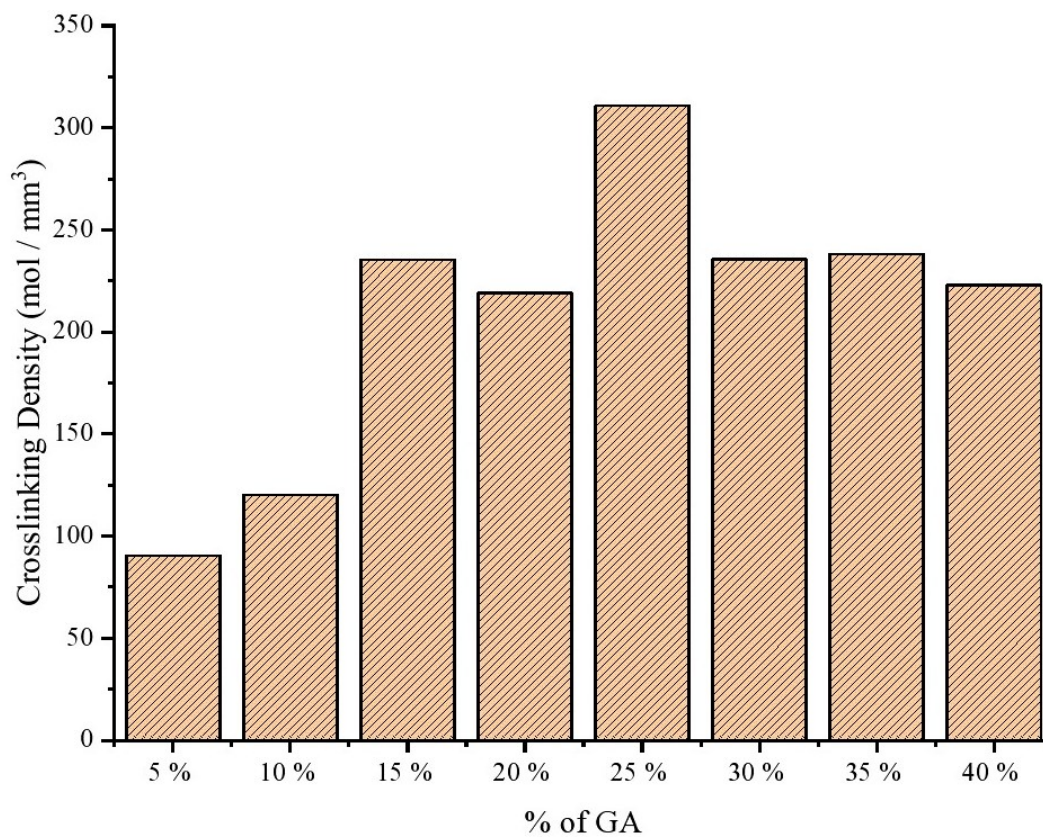
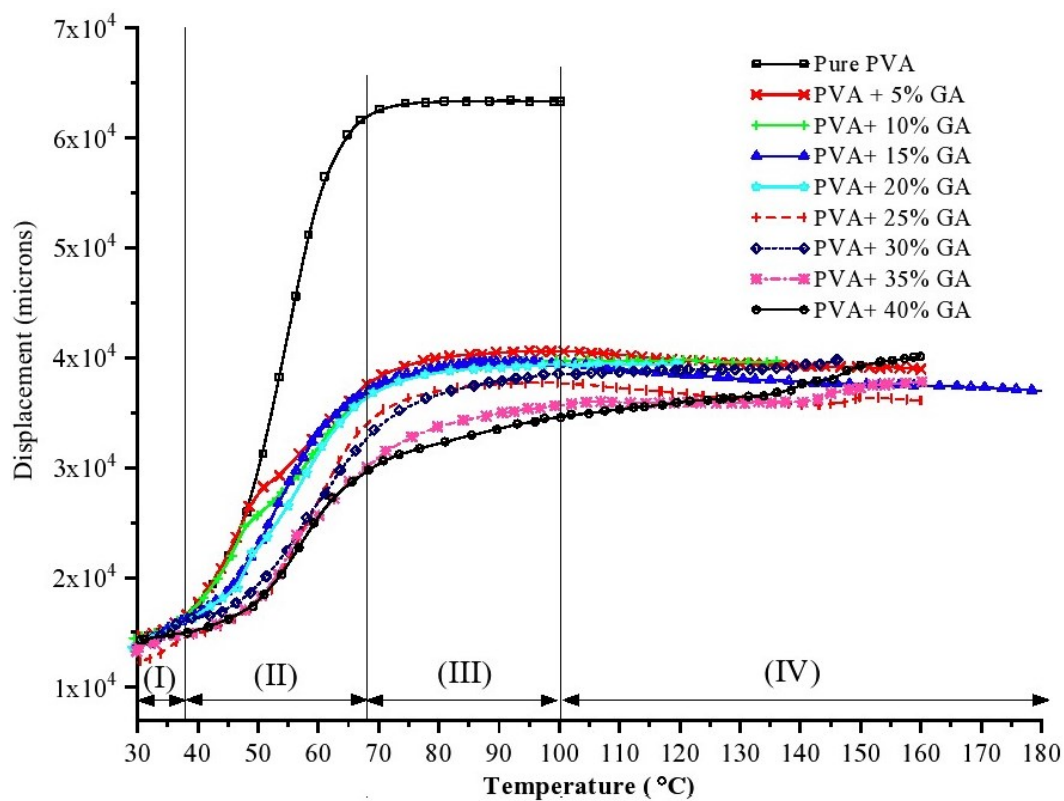
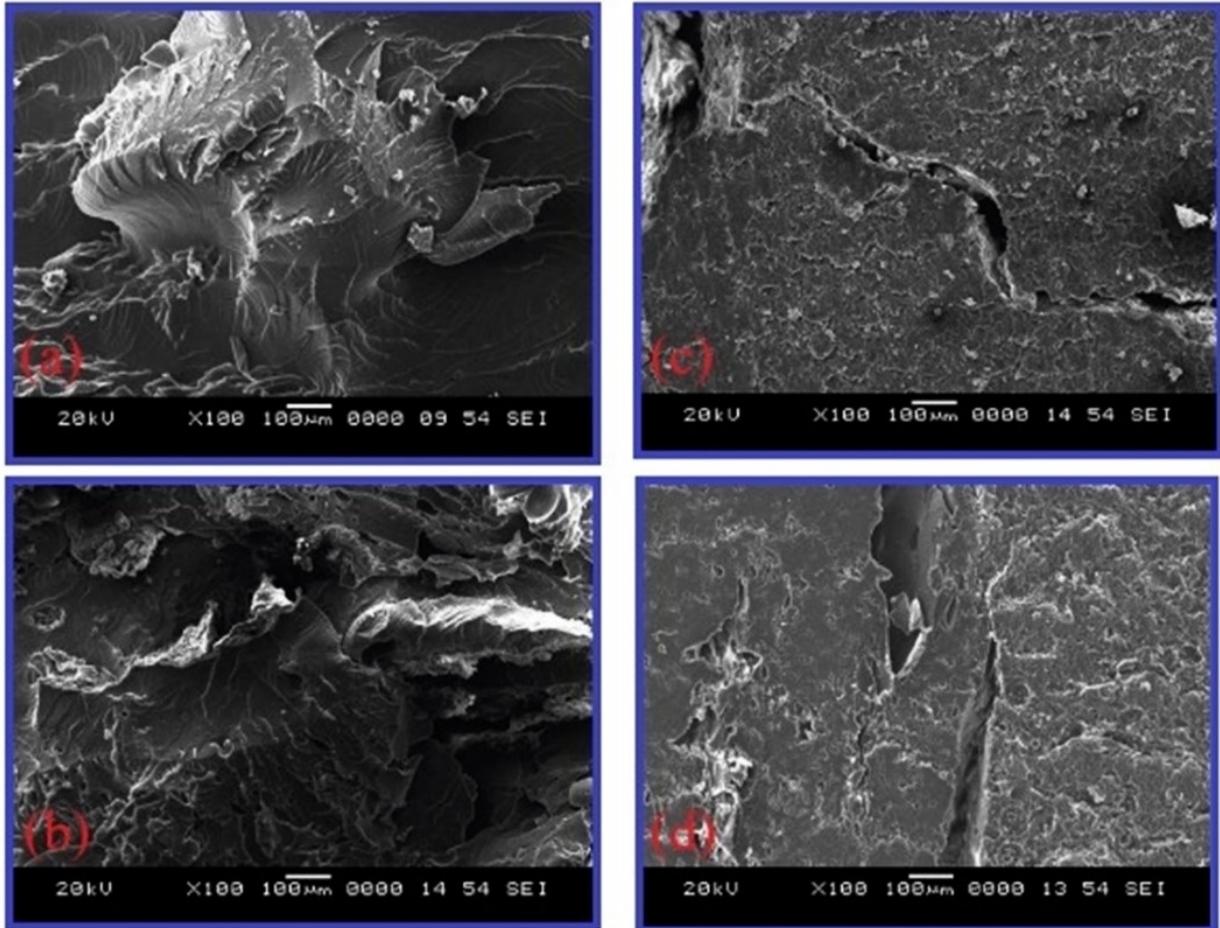


Figure 10. Effect of deflection with temperature for PVA-GA polymer



**Figure 11.** SEM images a) 15% GA in PVA b) 20% GA in PVA c) 30% GA in PVA and d) 40% GA in PVA



**Figure 12.** SEM images a) Neat PVA b) 20% GA in PVA c) 30% GA in PVA and d) 40% GA in PVA

